Investigation of fast particle driven instabilities by 2D Electron Cyclotron Emission Imaging on ASDEX Upgrade

IGJ Classen[1], Ph Lauber[2], D Curran[3], JE Boom[1], BJ Tobias[4], CW Domier[5], NC Luhmann Jr.[5], HK Park[6], M Garcia Munoz[2], B Geiger[2], M Maraschek[2], MA Van Zeeland[7], S da Graça[8] and the ASDEX Upgrade Team[2]

[1]FOM Institute for Plasma Physics Rijnhuizen, 3430 BE Nieuwegein, The Netherlands
[2]Max Planck Institut für Plasmaphysik, 85748 Garching, Germany
[3]Department of Physics, University College Cork, Cork, Ireland
[4]Princeton Plasma Physics Laboratory, Princeton, New Jersey, USA
[5]University of California-Davis, California, USA
[6]Pohang University of Science and Technology, Pohang, Republic of Korea
[7]General Atomics, P.O. Box 85608, San Diego, California, 92186-5608 USA
[8]Instituto de Plasma e Fusão Nuclear, P-1049-001 Liboa, Portugal

E-mail address: ivo.classen@ipp.mpg.de

Abstract. Detailed measurements of the 2D mode structure of Alfvén instabilities in the current ramp up phase of neutral beam heated discharges were performed on ASDEX Upgrade, using the electron cyclotron emission imaging (ECEI) diagnostic. This paper focuses on the observation of reversed shear Alfvén eigenmodes (RSAEs) and bursting modes that, with the use of the information from ECEI, have been identified as beta induced Alfvén eigenmodes (BAEs). Both RSAEs with first and second radial harmonic mode structures are observed. Calculations with the linear gyro-kinetic code LIGKA revealed that the ratio of the damping rates and the frequency difference between the first and second harmonic modes strongly depends on the shape of the q-profile. The bursting character of the BAE type modes, which are radially localised to rational q surfaces, is observed to sensitively depend on the plasma parameters, ranging from strongly bursting to almost steady state.

1. Introduction

In fusion plasmas, Alfvén instabilities can be driven unstable by a population of suprathermal energetic particles [1]. These instabilities can lead to an enhanced transport or complete loss of the fast particles. In ITER, it is expected that Alfvén instabilities are driven unstable by the 3.5 MeV alpha particles resulting from the D-T reactions, as well as by neutral beam injected (NBI) fast ions and ions accelerated by ion cyclotron resonance heating [2]. As the confinement of alpha particles is crucial for the performance of a burning plasma, it is important to understand the physics of Alfvén instabilities.

This paper presents measurements of Alfvén instabilities performed on the ASDEX Upgrade tokamak with the electron cyclotron emission imaging (ECEI) diagnostic [3]. ECEI gives a local, high resolution, 2D measurement of the electron temperature fluctuations associated with the Alfvén instabilities, accurately revealing their mode structure and position. Two distinct types of Alfvén instabilities are observed in the current ramp up phases of NBI heated plasmas; reversed shear Alfvén eigenmodes (RSAEs, also sometimes referred to as Alfvén cascades) and beta induced Alfvén eigenmodes (BAEs). The observed 2D mode structures and frequencies are compared to the theoretical predictions of the gyro-kinetic LIGKA code [4].

One of the main open questions concerning Alfvén instabilities is the non linear evolution of the mode amplitude. Various types of behavior, ranging from a steady state amplitude to an explosive growth, are predicted [5], and the type of behavior is expected to greatly influence the impact of the instabilities on the fast particle transport. The BAE modes reported in this paper are observed to make a transition from almost steady state to bursting.
Although this paper solely deals with the ASDEX Upgrade ECEI results, related experiments, yielding data on RSAEs, have recently been conducted using an ECEI diagnostic on DIII-D [6].

2. Electron Cyclotron Emission Imaging; diagnostic and data analysis

The 2D ECEI diagnostic [3] on ASDEX Upgrade (AUG, major radius R=1.65m, minor radius a=0.5m) provides a localized, high resolution 2D measurement of the electron temperature and its dynamics. The principle of a 2D ECEI diagnostic is comparable to a standard 1D heterodyne ECE radiometer, except that multiple lines of sight (16 on AUG) are simultaneously quasi-optically imaged onto a linear array of (16) diode detectors. Each of the lines of sight is treated as a 1D ECE radiometer, measuring the ECE intensity in a number of frequency bands (8 on AUG). This results in a direct 2D measurement of the electron temperature in a 2D array of 8 (horizontal) by 16 (vertical) positions (128 channels total) in the poloidal plane, covering an area of typically 10 by 40 cm. The position of this measurement area can be adjusted horizontally by tuning the diagnostic to different frequencies, simultaneously shifting the position of one of the lenses to adjust the position of the focal plane. For the experiments described in this paper, the system was tuned to measure just to the low field side of the plasma centre (range R=1.70-1.85m) as indicated in figure 1, and the data were sampled at 1 MHz.

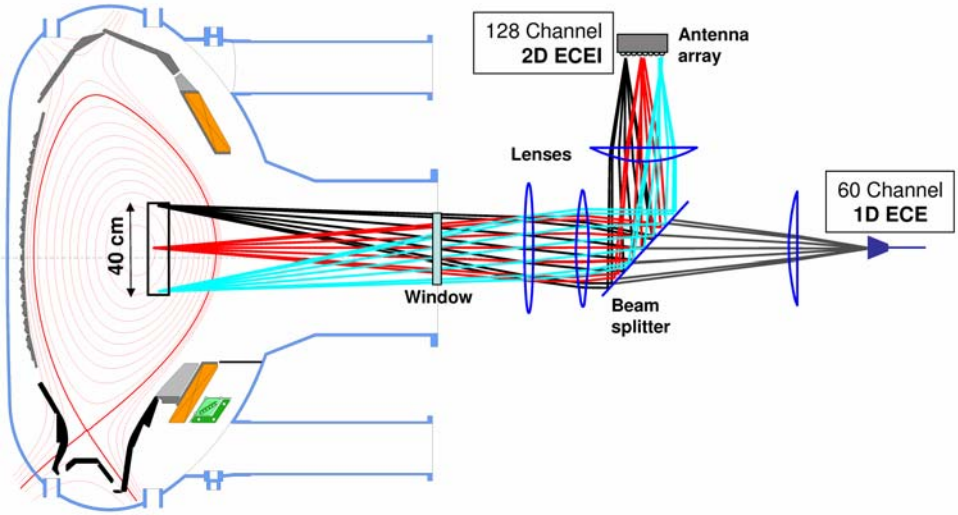

Figure 1. Overview of the ASDEX Upgrade ECEI system. The 16 lines of sight (3 are shown) are imaged onto an antenna array. The electron temperature is measured at 8 positions along each line of sight, giving 128 channels in an 8 by 16 array in the poloidal plane. Part of the ECEI optics is shared with a 60 channel 1D ECE radiometer.

In the optically thick plasmas under consideration, ECEI directly measures the (relative) electron temperature fluctuations $\delta T_e/T_e$. However, the accuracy of any ECE diagnostic is limited by thermal noise, which in these experiments amounts to a relative noise level of about 3%. The relative temperature fluctuations associated with Alfvén eigenmodes are typically 1%, so significantly below the noise level. To overcome this noise, the data has to be filtered. The data presented in this paper are subsequently filtered using (truncated) singular value decomposition (SVD) filtering and Fourier frequency selection. The SVD filtering enhances the coherent data content (fluctuations present on most channels simultaneously) and filters out most of the (incoherent) noise. The Fourier filtering drastically reduces the bandwidth of the signals, greatly reducing the thermal noise. Both filtering procedures are described in more detail in [3]. After filtering, direct observation of small amplitude fluctuations like the RSAEs is possible. For the weakest modes, a further averaging of the mode structure over time was required.

3. Shot overview

A series of shots with strong Alfvén activity has been analyzed. Basically, two types of modes were observed: RSAEs (implying a reversed shear q-profile) when NBI heating was applied early, and bursting BAE modes associated with the q=2 and q=1.5 surfaces. Variation of magnetic field, NBI timing and NBI beam energy led to significant differences in the MHD signature of these modes. In this paper, a discharge (25506) in which both the RSAEs and the BAE are strong is taken as the prime example. In this discharge 2.5MW of NBI power was applied early in the current ramp up phase at 0.22s (see figure 7 for NBI power and plasma current time traces). The injected deuterium atoms had an energy of 93 keV. The current ramp up phase of this discharge was identical to the discharges previously described in [7-9]. The toroidal magnetic field B_T was 2.0T. The shot was performed shortly after a boronisation to keep the electron density n_e low (line averaged n_e around $2{\cdot}10^{19}$ m^{-3}) to achieve a higher fast particle pressure fraction. Time traces of the line integrated n_e and the central T_e can be found in figure 7. Within the measurement uncertainty, T_i was equal to T_e.

Figure 2 gives an overview of the modes during the current ramp up phase, as observed by ECEI and magnetic pick up coils. The ECEI spectrogram (averaged over all available ECEI channels) shows Alfvén cascades dominating the spectrum before t=0.43s, and bursting (BAE) modes afterwards. So the q-profile has an off axis minimum at least up to 0.43s. The toroidal mode number n (middle plot) is derived from the phase relations between 6 toroidally distributed magnetic pick up coils (negative mode numbers represent modes rotating in the ion diamagnetic or co-current direction). Bursting BAEs (at about 60kHz) and steady state TAEs (at about 120 kHz) are seen to occur simultaneously. The fact that the TAEs are only seen in magnetics indicates that the TAEs are probably located at a larger minor radius, outside of the ECEI observation range. The radii of the various modes (relative to the radius of the plasma centre), derived from the 2D mode structure measured by ECEI, are shown in the bottom plot as function of time.

From the spectrogram, toroidal mode number n from magnetics, the (approximate) poloidal mode number m from ECEI and the radius of the modes, the evolution of the q-profile can be accurately derived [10]. The q-profile (with off axis minimum q_{min} at R_{qmin}) drops over time to lower values due to current diffusion. Indicated in figure 2 are the most prominent q_{min} crossings and the time at which the q=1.5 surface enters the plasma. Knowing that RSAEs are located at R_{qmin}, and that the BAEs are located close to rational surfaces, the mode radii can be attributed to these surfaces. R_{qmin} is observed to get smaller, and the radius of the q=2 and 1.5 surfaces increases as expected.

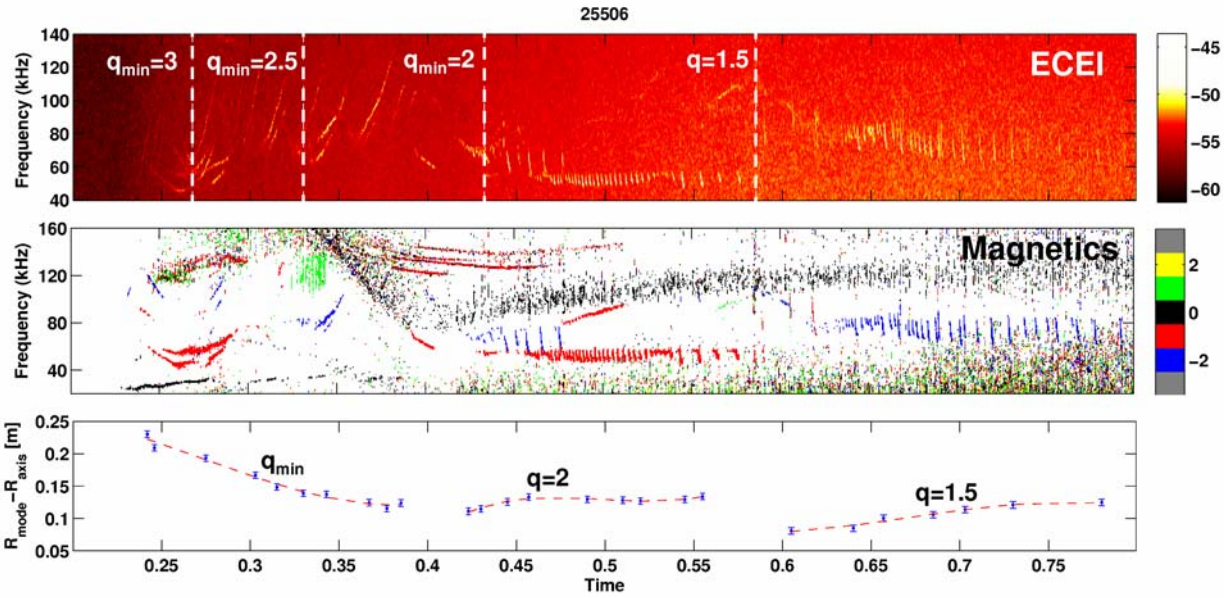

Figure 2. Overview of AUG shot 25506. The spectrogram from ECEI at the top shows the various Alfvén modes during the current ramp up phase. Indicated are the most prominent q_{min} crossings. Alfvén cascades dominate the spectrum before the q_{min}=2 crossing. Afterwards, bursting modes are observed. The middle plot gives the toroidal mode number n, derived from magnetics. The radius of the minimum in q (R_{qmin}) and of the q=2 and q=1.5 surfaces as function of time, derived from the 2D mode structure from ECEI, are shown at the bottom.

4. Modeling using the LIGKA code

The modes observed in shot 25506 have been modeled using the LIGKA [4] code. LIGKA is a linear, gyro-kinetic code to calculate the eigenmodes and damping/growth rates of Alfvén waves in realistic tokamak geometry. It relies on an accurate equilibrium reconstruction, for which the CLISTE code [11] has been used. The background electrons and ions as well as the fast particles are treated kinetically and their orbit information is taken from HAGIS [12]. The equilibrium determines both the Alfvén mode spectrum, calculated by LIGKA, and the fast particle orbits, provided by HAGIS.
Figure 3 shows the evolution of the Alfvén continuum, calculated by LIGKA, around the time that q_{min} drops below 2 (around 0.45s in shot 25506). As soon as the q-profile drops below 2, a local maximum in the continuum forms at radius R_{qmin}, that rapidly goes up in frequency as the q-profile drops further. The RSAEs are localized just above this maximum, explaining the frequency chirping. Simultaneously as q drops below 2, a local minimum is formed at the q=2 surface. The BAEs are localized just below this minimum and move radially out as the radius of the q=2 surface increases over time, leaving their frequency almost constant.

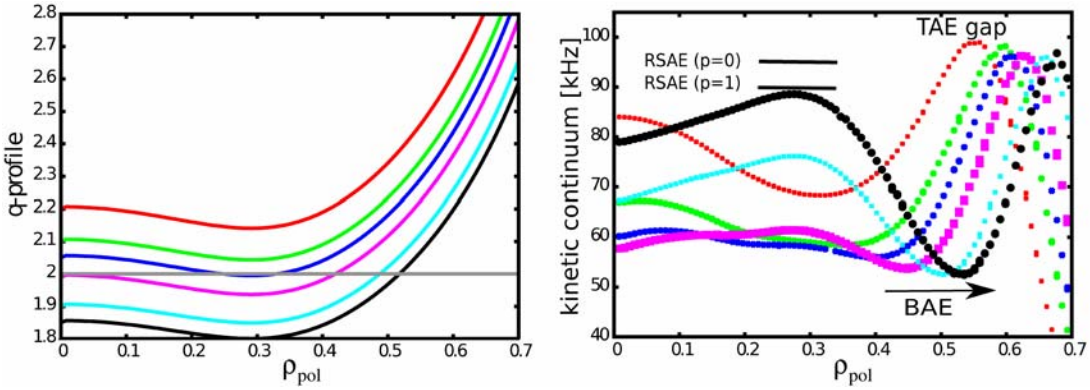

Figure 3. The evolution of the q-profile around the q_{min}=2 crossing (q dropping with time), and the associated kinetic Alfvén continua. RSAEs occur just above the maximum at the position of the q minimum. BAEs occur in the BAE gap, just below the minimum associated with the q=2 surface.

5. Reversed shear Alfvén eigenmodes

RSAEs occur when an off axis minimum in the q-profile exists and sufficient drive from a fast ion population is present [13]. An m/n RSAE is located at R_{qmin}, with a frequency just above the local maximum in the Alfven continuum that forms when q_{min} is slightly smaller than m/n. As q_{min} successively crosses different rational values $q=m/n$, a whole spectrum of RSAEs with different mode numbers is triggered (not to be confused with high n 'tearing mode cascades' reported earlier from ASDEX Upgrade [14], which have a different mode number evolution). When low order rational q values (q=3, 2.5, 2) are crossed, multiple modes with different mode numbers are simultaneously triggered, making it easy to identify such a crossing from a spectrogram. Before such a crossing, often down-chirping modes are observed (see figure 2), so called quasi-modes. An m/n quasi mode is located beneath the local minimum in the continuum at R_{qmin}, that forms when q_{min} is slightly above m/n. The frequency of an m/n RSAE chirps up as q_{min} drops below m/n. Neglecting plasma pressure, the frequency chirping of m/n RSAEs, starting at zero frequency, is described by [1]:

$$\omega_{AC}(t) \approx \left| \frac{m}{q_0(t)} - n \right| \frac{V_A}{R_0} \qquad (1)$$

where $V_A = B/\sqrt{\mu_0 \rho}$ is the Alfvén velocity and ρ is the mass density of the plasma. However, at finite pressure the BAE gap is formed, and equation 1 is altered to [15]:

$$\omega_{AC}(t) \approx \left[\left(\frac{m}{q_0(t)} - n \right)^2 \frac{V_A^2}{R_0^2} + \frac{2T_e}{M_i R_0^2} \left(1 + \frac{7}{4} \frac{T_i}{T_e} \right) \right]^{1/2} \qquad (2)$$

with the minimum frequency of the RSAEs now given by the geodesic frequency. In the lab-frame, a further correction is needed for the toroidal rotation frequency $\omega_{rot}=v_{rot}/R_0$. This correction is $n\cdot\omega_{rot}$, separating modes with different toroidal mode numbers in frequency.
Figure 4a shows a zoom of the ECEI spectrogram of figure 2, around the q_{min}=2.5 crossing. The mode labeled α is an m/n=5/2 RSAE, whose experimental 2D mode structure is shown in figures 4b and c. Figure 4b gives the amplitude A of the mode (about 1.5% relative temperature fluctuation), and figure 4c includes the phase information ($A\cos(\varphi)$), enabling an estimation of the poloidal mode number m. The simulated 2D mode structure of this mode, calculated by LIGKA, is shown in figure 4d, showing good agreement with experiment (measurement position of ECEI indicated by the white box). Also, the starting frequency and frequency evolution is nicely reproduced by LIGKA.
In experiment, often modes with a higher radial harmonic are observed [16], meaning the mode structure does not have a single maximum in radius as is the case for the mode shown in figure 4b, but two radial maxima are observed (it is located at two poloidal 'rings'). The mode labeled β in figure 4a, whose experimental mode structure is shown in figures 4e and f, is an example of such a mode. The LIGKA simulation for mode β is shown in figure 4g. Like the 1st radial harmonic mode α, also the 2nd radial harmonic mode β is an m/n=5/2 RSAE. The amplitudes of such 2nd harmonic modes are observed to be comparable to the associated 1st harmonic modes (about 1% for mode β). These 2nd harmonic modes are observed simultaneously with their 1st harmonic counterpart, but are always observed at a lower frequency. The frequency difference between modes α and β, Δf, is about 8kHz.

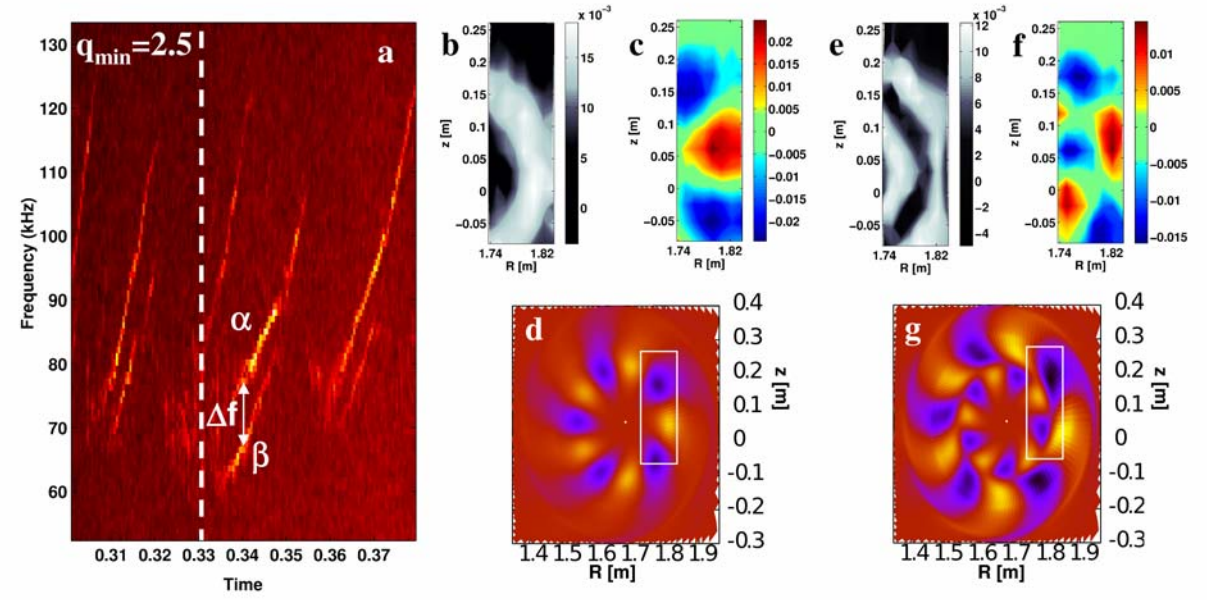

Figure 4. Figure a gives the ECEI spectrogram around the q_{min}=2.5 crossing showing various RSAEs. Figures b and c respectively show the 2D amplitude and mode structure ($A\cos(\varphi)$) of the 1st radial harmonic mode labelled α in figure a. The 2nd radial harmonic mode (β) is shown in figures e and f. The simulated mode structures from LIGKA are given in figures d and g.

LIGKA simulations showed that Δf depends on the exact shape of the q-profile. A strongly reversed q-profile results in a larger Δf than a shallow q-profile. Figure 5 shows the dependence of Δf on the q-profile shape (strongly reversed profiles characterized by a high second radial derivative of q at R_{qmin}), making Δf a possible diagnostic for the q-profile shape. Also the damping rate (γ_d/ω) for both the 1st and 2nd harmonic modes (here labeled p=0 and p=1 respectively) is plotted as a function of the q-profile shape, showing that a shallow q-profile favors the 2nd radial harmonic modes. For the q-profile shape belonging to the experimentally observed Δf of about 8kHz, the corresponding damping rates for modes α and β are equal (about 2%), explaining the equal mode amplitudes. These calculations used the experimental T_e, T_i and n_e profiles shown in figure 5. Different kinetic profiles might influence the calculation of Δf [17] [18].

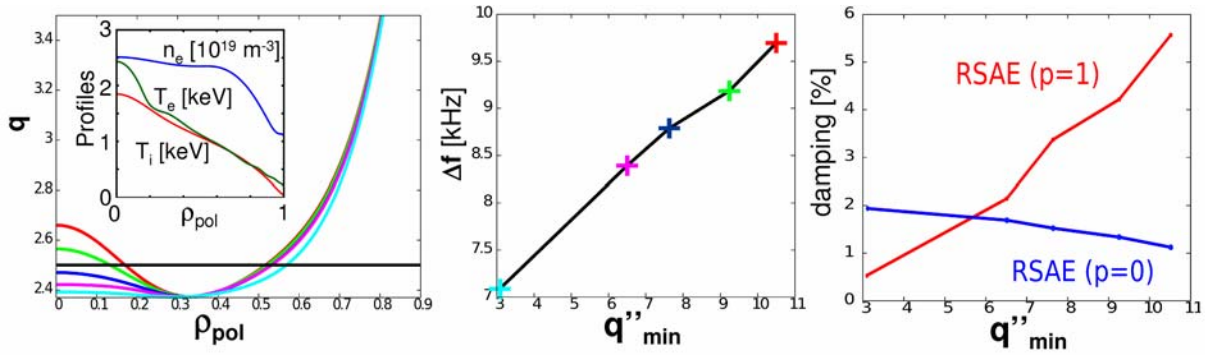

Figure 5. The frequency difference Δf between the 1st and 2nd radial harmonics of the m/n=5/2 RSAE is calculated to depend on the shape of the q profile. For the q profiles shown left (and the experimental n_e, T_e and T_i profiles shown in the inset), the calculated Δf is given at the right. So, strongly inversed q profiles (high second radial derivative of q at R_{qmin}) show a larger Δf. The experimentally observed value of Δf is around 8 kHz. The calculated damping rates for both harmonics (1st harmonic labelled p=0, 2nd harmonic p=1) are shown at the right.

6. Beta induced Alfvén eigenmodes

Figure 6a shows a spectrogram of the bursting modes associated with the q=2 surface, around 60kHz. The modes are observed to chirp down in frequency by as much as 15kHz (25% of their frequency). These modes are also observed by the fast ion loss detector (FILD) [19], as seen in the spectrogram in figure 6b, confirming that they cause an enhanced transport of fast particles. The 2D structures of the modes α-δ (indicated in figure 6a) are shown in figures 6c-f respectively. All modes are clearly observed to be radially localized (they form a 'ring' in the poloidal plane), with mode amplitudes (relative temperature fluctuation) up to 2.5%. This relative mode amplitude of 2.5% corresponds to a perpendicular displacement ξ of about 1 cm (neglecting compression effects, and assuming an experimental electron temperature gradient length of 0.4 m, approximately constant over the observation volume). The mode structure is not seen to change noticeably (within diagnostic error) during a burst. Estimating the mode numbers from both magnetics (figure 2) and ECEI, these modes are identified as either m/n=4/2 (α and β) or 2/1 (γ and δ). The location of the modes is seen to move radially outward with time, indicating that the modes are probably located at the (outward moving) q=2 surface. Mode α is likely a (remnant of a) quasi-mode, chirping down in frequency just before the q=2 surface enters the plasma, and is hence expected to be located at R_{qmin}. The onset frequencies of the other 4/2 (β) and 2/1 modes (γ and δ) are seen to stay constant (compare with figure 3). The onset frequency of the 2/1 modes is well explained by the geodesic frequency, corrected for the toroidal rotation f_{rot}, the 4/2 onset frequency is slightly too high. In some discharges, these modes are observed simultaneously with RSAEs, in others they occur with no RSAE activity. So, these modes can occur both with reversed and monotonous q-profiles.

The appearance of these modes in the spectrogram might lead to the conclusion that these are fishbones. Fishbones are however normally only associated with the q=1 surface and their mode structure would fill the entire plasma centre inside q=1 (it would not have a 'ring-like' mode structure). Previously reported m=2 fishbones [20] are located between the two q=2 surfaces in reversed shear profiles with q_{min} slightly below 2. The bursting modes observed here are seen to radially move out, contradicting that these modes are m=2 fishbones located between the two q=2 surfaces (one of them moving inward). All the above observations (i.e. mode frequency, radial location and radial structure) point in the direction that these modes (at least the 2/1 modes) should be interpreted as BAEs [21-23], localized below the local minimum associated with the rational q surface in the Alfvén continuum. These modes might be the same as the bursting modes reported in [24] and [25] (where they were referred to as 'high frequency fishbones').

Modeling of the 2/1 mode with LIGKA confirmed the mode (onset) frequency of 55kHz and calculated a damping rate of 2.2%. However, the simulated mode structure, calculated without fast particles, deviates significantly from the experimental one, indicating a strong influence of the fast particle distribution on the mode structure. LIGKA could not find a solution for the 4/2 mode, possibly

indicating that this mode is an energetic particle mode, also evidenced by the high onset frequency of the mode, which is above the continuum (chirping down through the continuum into the BAE gap).

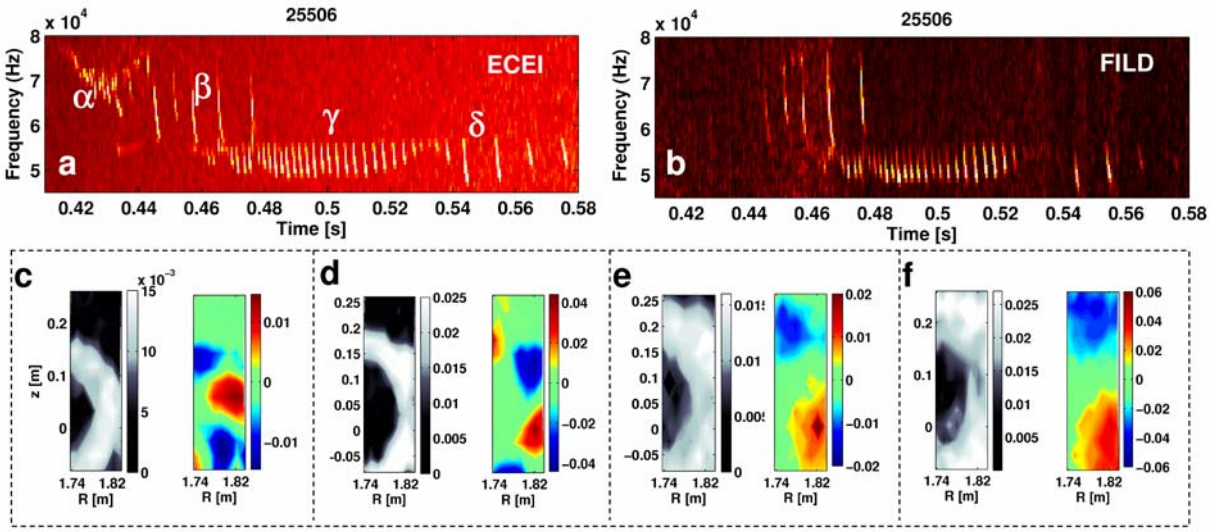

Figure 6. a) ECEI spectrogram showing the bursting BAE modes associated with the q=2 surface. b) These modes are also observed by the fast ion loss detector. Figures c-f show the 2D mode structures of the selected modes α-δ respectively (in pairs of left the amplitude A and right $A\cos(\varphi)$). Modes α and β are 4/2 modes, modes γ and δ are 2/1 modes. The position of the modes is seen to move radially outward with time.

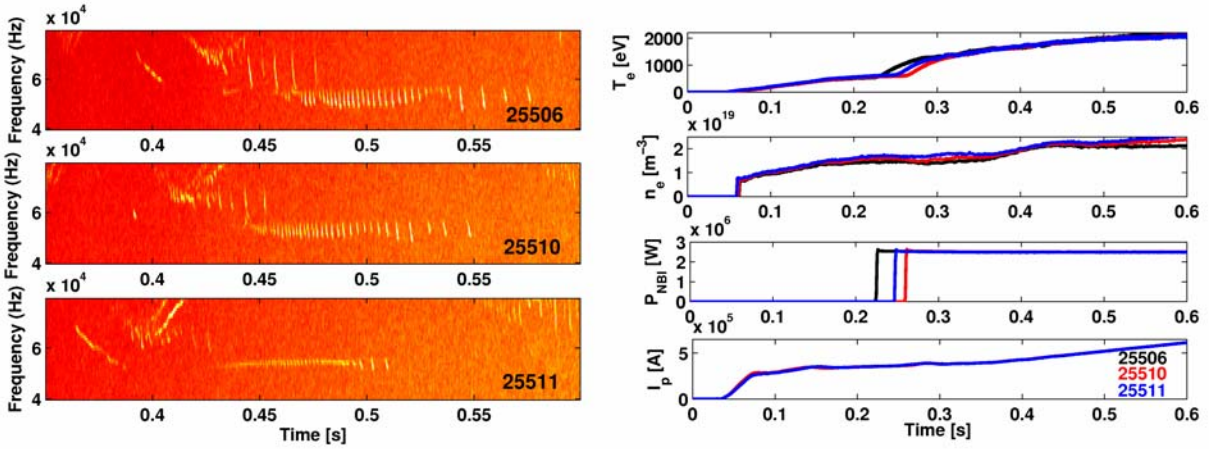

Figure 7. Spectrograms of AUG shots 25506, 25510 and 25511, showing differences in the bursting behaviour of the m/n=2/1 BAEs. The mode in shot 25511 is almost steady state. The three shots were almost identical, except for minor differences in central T_e (within error bars T_i=T_e), line averaged n_e and the NBI timing. The I_p ramps were identical.

The BAE modes have been observed in many discharges with early NBI heating. Figure 7 shows the spectrograms of three discharges with a clear change in the bursting behavior of the modes. All three discharges are very similar, except for small differences in temperature, density and NBI timing. Whereas the modes in discharges 25506 and 25510 show a clear bursting behavior, the 2/1 BAEs in discharge 25511 are almost steady state i.e. much shorter burst intervals and much less frequency change in single chirps. The only plasma parameter that is notably different at the time of the modes is the density. It is well known that a higher background density increases the background damping of Alfvénic modes. Therefore, the difference between linear drive and damping $\gamma = \gamma_L - \gamma_d$ becomes smaller. According to the non-linear theory developed in [26], the transition between the steady-state and bursting (explosive) regimes depends on the parameter $\hat{\nu} = \nu/\gamma = \nu/(\gamma_L - \gamma_d)$, where ν describes the relaxation process that tries to restore the original energetic particle distribution function on a time

scale $1/\nu$. If the density increases, γ_d becomes larger (γ smaller) and also (with constant ν) $\hat{\nu}$ increases. For larger $\hat{\nu}$ the analytical theory predicts the system to move towards steady state, which is seen in the experiment.

7. Conclusions and Outlook

The 2D ECEI diagnostic can greatly contribute to the research on Alfvén eigenmodes by accurately providing information like the 2D poloidal mode structure and radial position of these modes. On ASDEX Upgrade, both RSAEs and BAEs are observed during the current ramp up phase of early NBI heated discharges. Both 1st and 2nd radial harmonic RSAEs of comparable amplitude are observed, with the 2nd harmonic modes downshifted in frequency. The 2D mode structure and frequency splitting of the 1st and 2nd radial harmonic modes was reproduced by the linear gyrokinetic code LIGKA, and it was found that the frequency splitting is an experimental measurement of *q*-profile shape.

Bursting modes with a 'ring-like' poloidal mode structure are identified as BAE modes, located at rational *q* surfaces, moving radially out with these surfaces as the *q*-profile evolves. Modelling showed that the fast particle population has a strong influence on the mode structure (in case of the 2/1 modes) or even the existence (4/2) of these modes. The bursting character is experimentally seen to sensitively depend on the exact plasma parameters, ranging from strongly bursting to almost steady state. Lower density (smaller background damping) leads to more bursting modes, in accordance with theory.

Discharges with different magnetic field and beam energies have also recently been performed, showing significant differences in the appearance and bursting character of the BAE modes. Future work will concentrate on understanding and modeling these differences using HAGIS. Another topic of interest for future work is the transport caused by these modes. Data from the FILD [19] and FIDA [27] diagnostics on ASDEX Upgrade provide information on both the fast ion losses and fast ion distribution. The large amplitude of the bursting modes, and the fact that they can occur simultaneously with RSAEs at comparable radii, suggest a strong influence on the fast ion transport.

References

[1] Heidbrink WW 2008 *Physics of Plasmas* **15** 055501
[2] Fasoli A et al. 2007 *Nucl. Fusion* **47** S264
[3] Classen IGJ et al. 2010 *Rev. Sci. Instrum.* **81** 10D929
[4] Lauber PH, Günter S, Könies A and Pinches SD 2007 *J. Comp. Phys.* **226** 447-65
[5] Lilley MK, Breizman BN and Sharavov SE 2009 *Phys. Rev. Lett.* **102** 195003
[6] Tobias BJ, Classen IGJ, Domier CW, Heidbrink WW, Luhmann Jr. NC, Nazikian R, Park HK, Spong DA and Van Zeeland MA 2011 *Phys. Rev. Lett.* **106** 75003
[7] Garcia-Munoz M et al. 2010 in *Proceedings of 23rd Fusion Energy Conference Deajon, Korea* (IAEA, Vienna), Vol. IAEA-CN-180, EXW/P7-07
[8] Garcia-Munoz M et al. 2011 "Fast Ion Transport Induced by Alfvén Eigenmodes in the ASDEX Upgrade Tokamak" submitted to *Nucl. Fusion*
[9] Van Zeeland MA et al. 2011 *Physics of Plasmas* **18** 056114
[10] Sharapov SE et al. 2002 *Physics of Plasmas* **9** 2027-36
[11] Mc Carthy PJ 1999 *Physics of Plasmas* **6** 3554-60
[12] Pinches SD et al. 1998 *Comp. Phys. Comm.* **111**, 133-49
[13] Berk HL, Borba DN, Breizman BN, Pinches SD and Sharapov SE 2001 *Phys. Rev. Lett.* **87** 185002
[14] Gude A, Hallatschek K, Günter S, Kallenbach A, Pinches SD, Sesnic S and the ASDEX Upgrade Team 1998 *Plasma Phys. Control. Fusion* **40** 1057-71
[15] Breizman BN, Pekker MS, Sharapov SE and JET EFDA contributors 2005 *Physics of Plasmas* **12** 112506
[16] Van Zeeland MA et al. 2009 *Nucl. Fusion* **49** 065003
[17] Elfimov AG, Galvao RMO, Sharapov SE and JET-EFDA Contributors 2010 *Physics of Plasmas* **17** 110705
[18] Breizman BN and Sharapov SE 2011 *Plasma Phys. Control. Fusion* **53** 054001
[19] Garcia-Munoz M, Fahrbach H-U and Zohm H 2009 *Rev. Sci. Instrum.* **80** 053503
[20] Hender TC, Appel LC, Borba D, Huysmans GTA, Helander P, Kwon OJ and Sharapov S 1998 *Theory of Fusion Plasmas* **18** 307-17
[21] Zonca F, Chen L and Santoro A 1996 *Plasma Phys. Control. Fusion* **38** 2011-28
[22] Turnbull AD, Strait EJ, Heidbrink WW, Chu MS, Duong HH, Greene JM, Lao LL, Taylor TS and Thompson SJ 1993 *Phys. Fluids B* **5** 2546-53
[23] Heidbrink WW, Strait EJ, Chu MS and Turnbull AD 1993 *Phys. Rev. Lett.* **71** 855-8

[24] Heidbrink WW, Ruskov E, Carolipio EM, Fang J, Van Zeeland MA and James RA 1999 *Physics of Plasmas* **6** 1147-61
[25] Zonca F, Chen L, Botrugno A, Buratti P, Cardinali A, Cesario R, Pericoli Ridolfini V and JET-EFDA contributors 2009 *Nucl. Fusion* **49** 085009
[26] Berk HL, Breizman BN and Pekker M 1996 *Phys. Rev. Lett.* **76** 1256-9
[27] Geiger B, Garcia-Munoz M, Heidbrink WW, McDermott RM, Tardini G, Dux R, Fischer R, Igochine V and the ASDEX Upgrade Team 2011 *Plasma Phys. Control. Fusion* **53** 065010